



Measurement of the top quark mass with the matrix element method using the lepton+jets 1 fb^{-1} data set

The DØ Collaboration
URL <http://www-d0.fnal.gov>
(Dated: March 8, 2007)

A measurement of the top quark mass in the lepton+jets final state using the matrix element method is presented. The purity of the lepton+jets sample is enhanced by the application of a neural net-based b -tagging technique. The data set used for this measurement corresponds to 0.9 fb^{-1} acquired by the DØ experiment in Run II of the Fermilab Tevatron Collider. In addition to the top quark mass, an overall scale factor for jet energy calibration is included in fits to data. This scale factor is constrained by the reconstructed (W) mass of jets from hadronic W -boson decay in the $t\bar{t}$ event and by the standard jet energy scale calibration on the photon+jet sample. The combination of the e +jets and μ +jets channels for the untagged analysis yields:

$$m_{\text{top}}(\text{untagged}) = 170.5 \pm 2.5(\text{stat} + \text{JES})_{-1.4}^{+1.4}(\text{syst}) \text{ GeV}.$$

The combination of the e +jets and μ +jets channels for the analysis where b -tagging information is used yields:

$$m_{\text{top}}(b\text{-tag}) = 170.5 \pm 2.4(\text{stat} + \text{JES})_{-1.2}^{+1.2}(\text{syst}) \text{ GeV}.$$

Preliminary Results for the Winter Conference, 2007

I. INTRODUCTION

In the framework of the Standard Model, the top quark decays to a W -boson and b -quark nearly 100% of the time. Top pair production data samples are classified according to W boson decay channels. The data set is referred to as “dilepton”, if both W bosons decay leptonically, “all jets”, if both W bosons decay hadronically and “lepton+jets”, if one of the W bosons decays leptonically and the other one hadronically. What is referred to as a “jet” is described in Ref. [1].

In this note we present an updated measurement of the top quark mass using 910 (e +jets) and 870 (μ +jets) pb^{-1} of $D\bar{O}$ data. Previous measurements of the top quark mass in the lepton+jets channel from $D\bar{O}$ are described in Ref. [2] and Ref. [3]. The current measurement uses the matrix element method described in Ref. [2]. This method is well established and has consistently yielded high precision results [4]. We do not intend to give a full overview of the method but will rather concentrate on what is new in this round of analysis. The main difference is a $2.5\times$ increase in the data set and significant improvements in the event reconstruction. The definition of the reconstructed objects, the data integrity requirements, and comparisons between data and Monte Carlo predictions for this data set are given in Ref. [6]. For this version of the analysis, a new b -tagging algorithm based on neural nets is used [7]. The performance of this algorithm on lepton+jets data was tested as part of a recent lepton+jets b -tagging cross section measurement [8]. The changes in the mass reconstruction method itself are

- the addition of an integration over the electron resolution (previously only the muon resolution was taken into account);
- an integration over the transverse momentum of the $t\bar{t}$ system, which was previously assumed to be equal to zero;
- the use of a prior to constrain the overall jet calibration (JES). Jet energies are constrained to the value derived on the photon+jets data set within its uncertainty, while the hadronic W -boson mass is used as an additional constraint. The prior was not used in the previous version of the analysis and the jet energy scale was determined only by the hadronic W -boson mass.

II. DATA SAMPLE AND SIMULATION

The selection of $t\bar{t}$ events is similar to the previous version of the analysis except that improved offline reconstruction is used [5]. Objects and sample composition were studied for the topological ℓ +jets $t\bar{t}$ cross section analysis described in Ref. [6] and in the b -tagging ℓ +jets $t\bar{t}$ cross section analysis described in Ref. [8].

The data sample corresponds to 910 (e +jets) and 870 (μ +jets) pb^{-1} of $D\bar{O}$ data. $t\bar{t}$ events were simulated with PYTHIA [9], followed by full $D\bar{O}$ detector simulation. The dominant W +jets backgrounds were generated by matched ALPGEN [10] in exclusive jet multiplicity bins, separately for each flavor composition. The MLM matching scheme was used. These separate samples were then added together with the appropriate event weights. Because of this feature, weighted simulated W +jets events were used in ensemble testing described later. The weights were used in deciding when to include (or not) an event in the ensemble. The QCD multijet background, in which a jet is misinterpreted as a lepton, is estimated from data samples in which leptons are required to pass loose selection, but fail tight requirements. For details, see [6].

III. FINAL SELECTION AND SAMPLE COMPOSITION

All events are required to pass the following kinematic selection criteria:

- exactly four jets with $p_T > 20$ GeV and $|\eta| < 2.5$;
- an isolated electron or muon with $p_T > 20$ GeV and $|\eta| < 2$ for muons or $|\eta| < 1.1$ for electrons;
- $\cancel{E}_T > 20$ GeV;

Rejecting events with more than four jets (in contrast to the cross section analyses) is motivated by the fact that a signal probability P_{sgn} is calculated using a first-order matrix element for $t\bar{t}$ production. Decays with additional radiation as well as $t\bar{t}$ pairs produced in association with other jets are not modeled in the probability. The exclusive four jets requirement minimizes the number of such events in the selected sample. A total of 251 e +jets and 256 μ +jets events are selected.

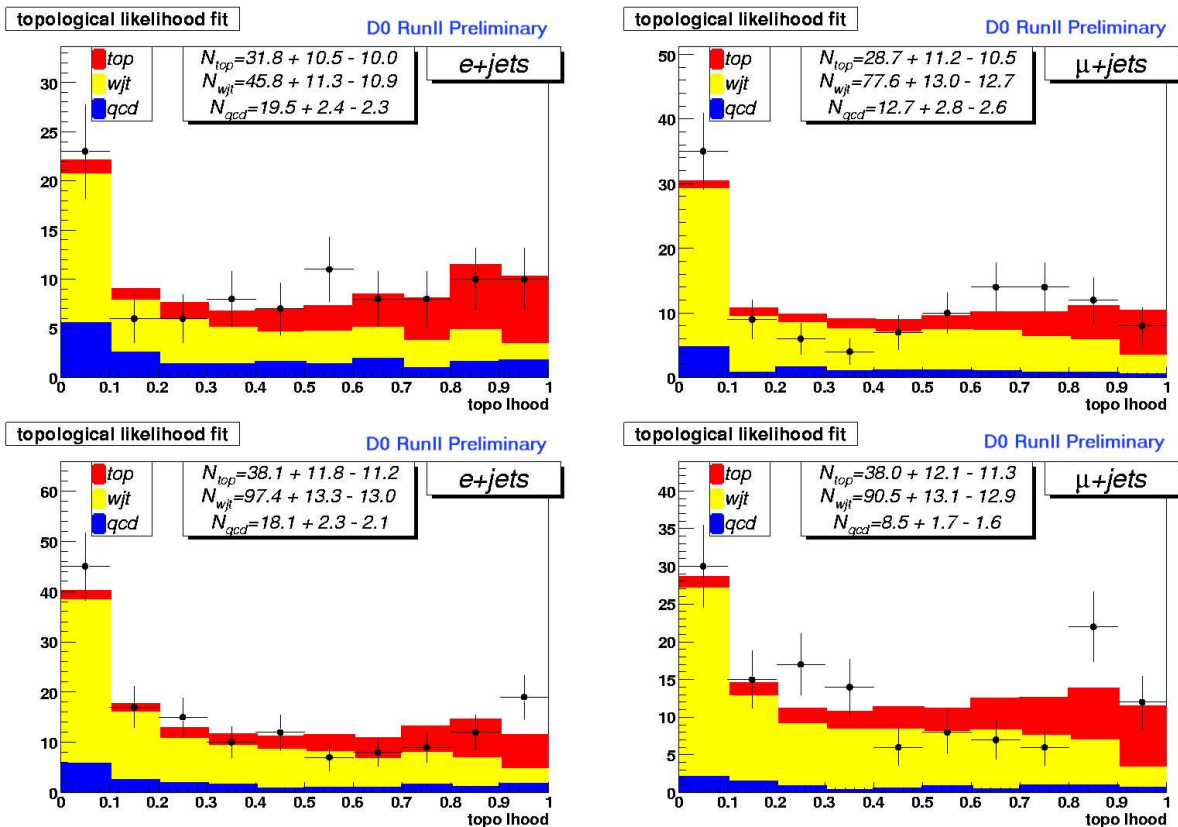


FIG. 1: Topological likelihood fit applied to the data sample. The two plots in the first and second rows are for pre-shutdown and post-shutdown data, respectively. Only statistical uncertainties are shown for the contribution of each component.

channel	N_{evts}	f_{top}	f_{Wjets}	f_{QCD}
$e+jets$	251	$27.6 \pm 6.2\%$	$57.3 \pm 6.8\%$	$15.1 \pm 1.3\%$
$\mu+jets$	256	$25.4 \pm 5.3\%$	$66.2 \pm 6.0\%$	$8.36 \pm 1.1\%$

TABLE I: Composition of the $e+jets$ and $\mu+jets$ data samples without b -tagging requirement estimated with the topological likelihood technique.

To determine the signal fraction to use in the ensemble tests, a likelihood discriminant based on topological variables is calculated for each selected event as described in [11]. A fit to the observed distribution then yields the fractions of $t\bar{t}$, $W+jets$, and QCD multijet events in the data sample, separately for $e+jets$ and $\mu+jets$ events. Data sets for run numbers earlier than 200,000 and later than 200,000 are referred to as “pre” and “post” shutdown respectively. The fits were performed separately because the shapes of the likelihoods for these two data taking periods were sufficiently different. The fits are shown in Figure 1, and the results are summarized in Table I. Note that the likelihood discriminant is only used to determine the fraction of signal and background events to use in the ensemble testing and does not enter the top quark mass fit.

The sample composition was analyzed before applying b -tagging. In this version of the analysis we use b -tagging information provided by the neural net b -tagger [7]. We use the “Medium” operating point, which corresponds to a cut on the neural net variable of 0.65.

IV. MEASUREMENT OF THE TOP QUARK MASS WITH THE MATRIX ELEMENT METHOD

In this section, the measurement of the top quark mass with the matrix element method is described. The method used here is similar to the one of Ref. [4]; however, the method now allows for a simultaneous measurement of the top quark mass and the jet energy scale.

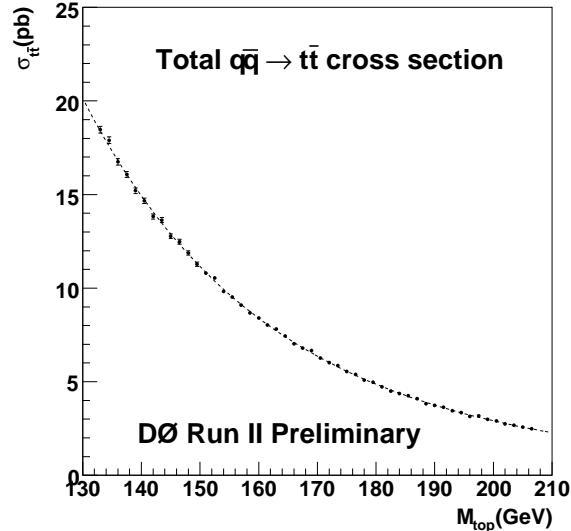


FIG. 2: The calculated total $t\bar{t}$ cross section as a function of the top mass used in the signal probability normalization.

An overview of the Matrix Element method is given in Section IV A. In Section IV B, the parameterization of the detector response is discussed. The mass fit and its calibration are described in Section IV C, and the result on data is given in Section IV D. Systematic uncertainties are discussed in Section V.

A. The Matrix Element Method

To maximize the statistical information on the top quark mass extracted from the event sample, a probability is calculated for each event as a function of the assumed top quark mass (m_{top}) and jet energy scale (JES). The probabilities from all events in the sample are then combined to obtain the sample probability as a function of assumed mass and jet energy scale, and the top quark mass measurement is extracted by finding the values that maximize this probability. The probability P_{evt} for one event is composed from probabilities for two processes, $t\bar{t}$ production and W +jets events, as

$$P_{\text{evt}}(x; m_{\text{top}}, JES, f_{\text{top}}) = f_{\text{top}} \cdot P_{\text{sgn}}(x; m_{\text{top}}, JES) + (1 - f_{\text{top}}) \cdot P_{\text{bkg}}(x) . \quad (1)$$

Here, x denotes the kinematic variables of the event (jets and leptons energies and angles), f_{top} is the signal fraction of the event sample, and P_{sgn} and P_{bkg} are the probabilities for $t\bar{t}$ and W +jets production, respectively. QCD background shape is assumed to be similar to that of W +jets and is not included in the background calculation. The effect of the difference in shapes between QCD and W +jets is accounted for in the systematic uncertainty.

The differential probability to observe a $t\bar{t}$ event with objects kinematics x in the detector is then given by

$$P_{\text{sgn}}(x; m_{\text{top}}, JES) = \frac{1}{\sigma_{\text{obs}}(p\bar{p} \rightarrow t\bar{t}; m_{\text{top}}, JES)} \times \sum_{\text{perm}} w_i \int_{q_1, q_2, y} \sum_{\text{flavors}} dq_1 dq_2 f(q_1) f(q_2) \frac{(2\pi)^4 |\mathcal{M}(q\bar{q} \rightarrow t\bar{t} \rightarrow y)|^2}{2q_1 q_2 s} d\Phi_6 W(x, y; JES) . \quad (2)$$

Here, the symbol \mathcal{M} denotes the matrix element for the process $q\bar{q} \rightarrow t\bar{t} \rightarrow b(\ell\nu)b(qq)$, s is the $p\bar{p}$ center-of-mass energy squared, q_1 and q_2 are the momentum fractions of the colliding partons (which are assumed to be massless) within the colliding proton and antiproton, and $d\Phi_6$ is an element of six-body phase space. $f(q)$ denotes the probability density to find a parton of given flavor and momentum fraction q in the proton or antiproton. The finite detector resolution is taken into account via a convolution with a transfer function $W(x, y; JES)$ that describes the probability to reconstruct a partonic final state y as x in the detector.

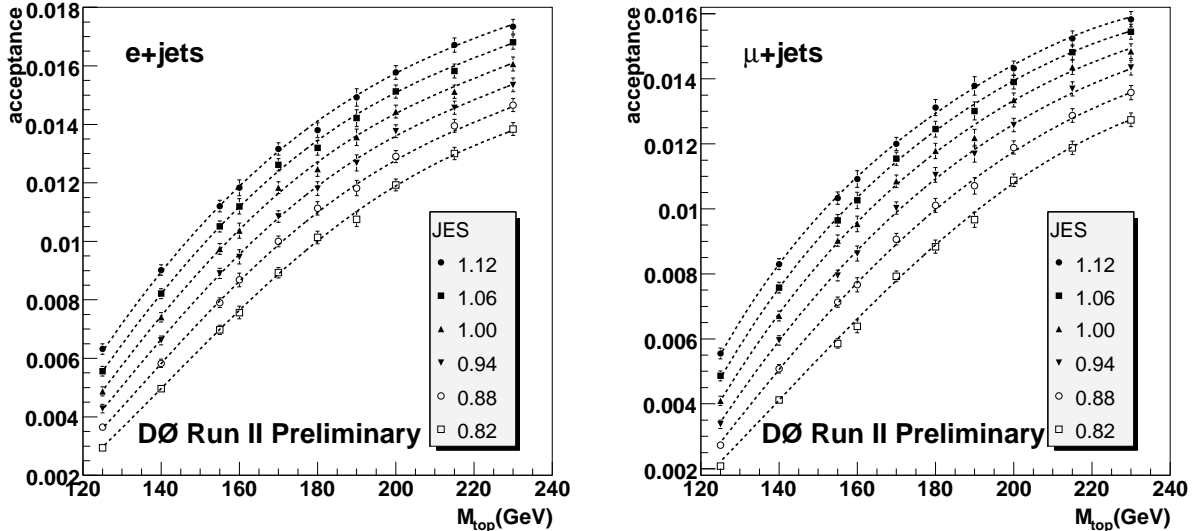


FIG. 3: The dependence of the overall acceptance on the top mass for e +jets (left) and μ +jets (right) samples.

Since it is not known which parton a jet comes from, a sum must be carried out over all 24 permutations of jet-to-parton assignments. w_i represents the weight of each permutation. For the untagged case, we have $w_i = 1/24$. For the b -tagging case, w_i is the normalized product of the probabilities of tagging each jet.

The corresponding overall detector efficiency depends both on m_{top} and on the jet energy scale. This is taken into account in the cross-section of $t\bar{t}$ events observed in the detector:

$$\sigma_{\text{obs}}(p\bar{p} \rightarrow t\bar{t}; m_{\text{top}}, JES) = \int_{q_1, q_2, x, y} d\sigma(p\bar{p} \rightarrow t\bar{t} \rightarrow y; m_{\text{top}}) W(x, y; JES) f_{\text{acc}}(x) \quad (3)$$

$$= \left\{ \int_{q_1, q_2, x, y} d\sigma(p\bar{p} \rightarrow t\bar{t} \rightarrow y; m_{\text{top}}) \right\} \times \frac{1}{M} \sum_{\text{acc}} (\text{event weight}) . \quad (4)$$

where M is the number of generated Monte Carlo events and the sum runs over all the events that pass the cuts, event reconstruction, etc. Due to trigger and some ID efficiencies, Monte Carlo events carry a weight. Therefore, the sum in Eq. 3 above is a sum of these weights for each event over all accepted events. The dependence of the total cross section on the top mass is presented in Fig. 2. The dependence of the overall acceptance on the top mass for e +jets and μ +jets samples is presented in Fig. 3.

The expression for the background probability P_{bkg} is similar to that for P_{sgn} given in Eq. 2 except that the VECBOS [14] parameterization of the matrix element \mathcal{M} is used and all jets are assumed to be light. Since the matrix element for W +jets production does not depend on m_{top} , P_{bkg} is independent of m_{top} and JES (see Section IV C).

In order to extract the top quark mass from a set of n measured events x_1, \dots, x_n , a likelihood function is built from the individual event probabilities calculated according to Equation (1) as

$$L(x_1, \dots, x_n; m_{\text{top}}, JES, f_{\text{top}}) = \prod_{i=1}^n P_{\text{evt}}(x_i; m_{\text{top}}, JES, f_{\text{top}}) . \quad (5)$$

For every assumed pair of values (m_{top}, JES) , the value of $f_{\text{top}}^{\text{best}}$ that maximizes the likelihood is determined. The top quark mass and jet energy scale are then obtained by projecting:

$$L(x_1, \dots, x_n; m_{\text{top}}, JES) = L(x_1, \dots, x_n; m_{\text{top}}, JES, f_{\text{top}}^{\text{best}}(m_{\text{top}}, JES)) \quad (6)$$

onto the m_{top} axis:

$$L(x_1, \dots, x_n; m_{\text{top}}) = \int L(x_1, \dots, x_n; m_{\text{top}}, JES) d(JES) . \quad (7)$$

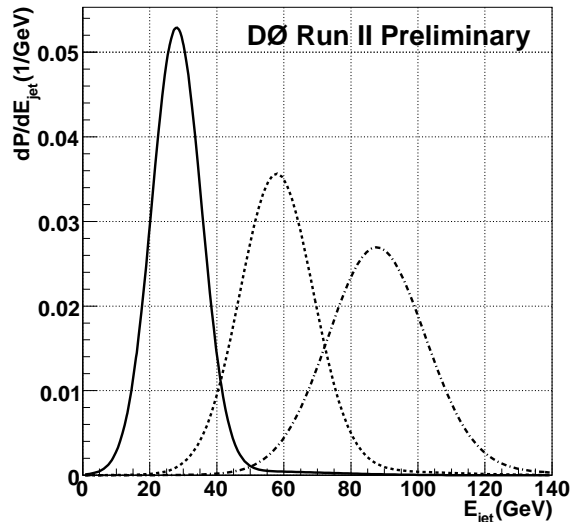


FIG. 4: Transfer functions for light quark jets for parton energies 30 (solid), 60 (dashed) and 90 (dashed-dotted) GeV in the central region, $|\eta| < 0.5$, and for the reference jet energy scale $JES=1.00$

The mean (or peak) and the rms (or width) of $L(x_1, \dots, x_n; m_{\text{top}})$ is then used to extract the best estimation of the top mass and its error. The projection given by Eq. 7 assumes no prior knowledge of the jet energy scale. If prior information of the JES is known (like the γ +jets analysis), then instead of the projection given by Eq. 7, we use:

$$L(x_1, \dots, x_n; m_{\text{top}}) = \int L(x_1, \dots, x_n; m_{\text{top}}, JES) G(JES) d(JES) \quad (8)$$

where the prior $G(JES)$ is a Gaussian function centered at $JES = 1$ having a width $\sigma = 0.037$ (see Section IV C).

When using b -tagging, the events are divided into three groups: 0, 1, and 2 or more b -tags. A likelihood like in Eq. 6 is calculated for each group with an f_{top} maximization performed independently for each group. After that, the likelihoods for all three groups are multiplied and projected onto the m_{top} axis according to Eq. 7 or Eq. 8 depending on whether a prior is used or not.

B. Description of the Detector Response

The transfer function $W(x, y; JES)$ factorizes into contributions from the individual $t\bar{t}$ decay products. The angles of all measured $t\bar{t}$ decay products are assumed to be well-measured; this reduces the dimensions of the integration over 6-particle phase space. In this section, the jet and electron energy and muon transverse momentum resolutions are discussed.

1. Parameterization of the Jet Energy Resolution

The transfer function for calorimeter jets, $W_{\text{jet}}(E_x, E_y; JES)$, yields the probability for a measurement E_x in the detector if the true quark energy is E_y . For the case $JES = 1$, it is parameterized as

$$W_{\text{jet}}(E_x, E_y; JES = 1) = \frac{1}{\sqrt{2\pi}(p_2 + p_3 p_5)} \left[\exp\left(-\frac{((E_x - E_y) - p_1)^2}{2p_2^2}\right) + p_3 \exp\left(-\frac{((E_x - E_y) - p_4)^2}{2p_5^2}\right) \right]. \quad (9)$$

The p_i are themselves functions of the quark energy, and are parameterized as linear functions of the quark energy, so that

$$p_i = a_i + E_y \cdot b_i, \quad (10)$$

parameter	with silicon hits		no silicon hits	
	<i>pre</i>	<i>post</i>	<i>pre</i>	<i>post</i>
$\sigma_0(0)$	1.800×10^{-3}	2.066×10^{-3}	2.665×10^{-3}	2.968×10^{-3}
$\sigma_0(1)$	1.604×10^{-2}	2.219×10^{-2}	1.392×10^{-2}	2.913×10^{-2}
$c_0(0)$	4.958×10^{-3}	5.557×10^{-3}	1.456×10^{-2}	1.649×10^{-2}
$c_0(1)$	9.085×10^{-2}	1.190×10^{-1}	5.826×10^{-2}	-3.035×10^{-2}
$\eta_0(0)$	1.4	1.4	1.4	1.4
$\eta_0(1)$	0.	0.	0.	0.

TABLE II: Muon transfer function parameters for pre-shutdown and post-shutdown data taking periods and for the cases with and without silicon hits associated to the μ tracks

with a_3 set to 0.

The parameters a_i and b_i are determined from simulated events, after all jet energy corrections have been applied. The parton and jet energies are fed to an unbinned likelihood fit that minimizes the product of W_{jet} for each event with respect to a_i and b_i . A different set of parameters is derived for each of four η regions: $|\eta| < 0.5$, $0.5 < |\eta| < 1.0$, $1.0 < |\eta| < 1.5$, and $1.5 < |\eta| < 2.5$, and for three different quark varieties: light quarks (u, d, s, c), b quarks with a soft muon tag in the associated jet, and all other b quarks.

For $JES \neq 1$, the jet transfer function is adapted as follows:

$$W_{jet}(E_x, E_y; JES) = \frac{W_{jet}\left(\frac{E_x}{JES}, E_y; 1\right)}{JES}. \quad (11)$$

The JES factor is needed in the denominator to preserve the normalization $\int W_{jet}(E_x, E_y; JES) dE_x = 1$. An example of Monte Carlo derived transfer functions for light jets is shown in Figure 4 for energies 30, 60 and 90 GeV and $JES=1$.

2. Parameterization of the Muon Momentum Resolution

To describe the resolution of the central tracking chamber, the resolution of the charge divided by the transverse momentum of a particle is considered as a function of pseudorapidity. The muon transfer function is parameterized as

$$W_\mu((q/p_T)^{\mu,x}, (q/p_T)^{\mu,y}) = \frac{1}{\sqrt{2\pi}\sigma} \exp\left(-\frac{1}{2} \left(\frac{(q/p_T)^{\mu,x} - (q/p_T)^{\mu,y}}{\sigma}\right)^2\right), \quad (12)$$

where q denotes the charge and p_T the transverse momentum of a generated (y) muon or its reconstructed (x) track. The resolution

$$\sigma = \begin{cases} \sigma_0 & \text{for } |\eta| \leq \eta_0 \\ \sqrt{\sigma_0^2 + [c(|\eta| - \eta_0)]^2} & \text{for } |\eta| > \eta_0 \end{cases}, \quad (13)$$

has been obtained from muon tracks in simulated events where the parameters above are a linear function of $1/p_T$:

$$\begin{aligned} \sigma_0 &= \sigma_0(0) + \sigma_0(1) \cdot 1/p_T \\ c_0 &= c_0(0) + c_0(1) \cdot 1/p_T \\ \eta_0 &= \eta_0(0) + \eta_0(1) \cdot 1/p_T. \end{aligned} \quad (14)$$

The values of the coefficients are given in Table II for pre-shutdown and post-shutdown data taking periods and for the cases where the μ tracks are associated with and without hits in the silicon tracker.

The muon charge is not used in the calculation of P_{sgn} and P_{bkg} . However, for muons with large transverse momentum it is important to take the possibility of charge misidentification into account in the transfer function.

3. Parameterization of the Electron Energy Resolution

The electron energy resolution is parameterized by the transfer function:

$$W_e(E_x, E_y) = \frac{1}{\sqrt{2\pi}\sigma} \exp\left[-\frac{1}{2}\left(\frac{E_x - E_y}{\sigma}\right)^2\right], \quad (15)$$

where:

$$\begin{aligned} E_x &= \text{reconstructed electron energy} \\ E_y &= 1.0002 \cdot E_{\text{true}} + 0.324 \\ \sigma &= \sqrt{(0.028 \cdot E_y)^2 + (S \cdot E_y)^2 + (0.4)^2} \\ S &= \frac{0.164}{\sqrt{E_y}} + \frac{0.122}{E_y} \exp\left(\frac{p_1}{\sin\{2 \arctan[\exp(-\eta_e)]\}}\right) - p_1 \\ p_1 &= 1.35193 - \frac{2.09564}{E_y} - \frac{6.98578}{E_y^2}. \end{aligned}$$

This parameterization was obtained from the $D\bar{O}$ W mass group [15].

C. Top Quark Mass Fit

For each measured event, the signal probability P_{sgn} is calculated as a function of two parameters: the top mass m_{top} and the Jet Energy Scale JES . In the calculation of the background probability P_{bkg} , the Jet Energy Scale is kept constant at $JES = 1$.

The parameter JES is used to adjust for a possible overall miscalibration of the Jet Energy Scale. For signal events, since the W mass is fixed in the signal matrix element, the likelihood as a function of JES will be maximal when the invariant mass of the two light jets gives the W mass. Therefore, the parameter JES will compensate for small overall miscalibrations in the energy of the jets by taking advantage of the W mass constraint. For background events, on the other hand, one either has leptonically decaying W 's (as in W +jets events) or none at all (as in QCD events). This means that the W mass constraint exists only in signal events. If one could distinguish between signal and background events, one would vary JES in the signal events and leave it constant in the background ones. Unfortunately this distinction cannot be done, so the best thing to do is to let events with a large $P_{\text{sgn}}/P_{\text{bkg}}$ ratio change the likelihood when JES is varied while making sure there is little or no change in the likelihood for events with a small $P_{\text{sgn}}/P_{\text{bkg}}$ ratio. In other words, background-like events should not be allowed to play a role in the JES calibration. Since the total probability is a sum of P_{sgn} and P_{bkg} , this is achieved by keeping JES constant in the calculation of the background probability.

The analysis was performed according to the prescription given in Section IV A. The top mass and width were extracted using Eqs. 6-8. The following three cases were considered, a) fixed jet energy scale (mostly $JES=1$), b) unconstrained JES (or flat prior like in Eq. 7), and c) the use of a Gaussian prior like in Eq. 8. Unless specified otherwise, the plots and results that follow were calculated using a jet energy prior.

The width of the prior ($\sigma = 0.037$) was calculated using the jet energy scale errors derived from a γ +jets sample by the $D\bar{O}$ Jet Energy Scale Group (JESG). The fractional errors provided by the JESG are plotted for each jet from a $t\bar{t}$ Monte Carlo sample in Fig. 5. The average of the fractional errors in this figure is used as the width of the JES prior.

For given values of JES and m_{top} , each event probability $P_{\text{evt}} = f_{\text{top}}P_{\text{sgn}} + (1 - f_{\text{top}})P_{\text{bkg}}$ depends on the signal fraction f_{top} , and consequently, the likelihood L for the whole event sample as given in Equation (5) is a function of f_{top} .

1. Validation of the Method

The method is first validated using the fully simulated Pythia $t\bar{t}$ signal events described in Section II in which all four jets in each event are required to be matched to partons.

Ensembles consist of 200 pure $t\bar{t}$ signal events (50% e +jets and 50% μ +jets) drawn from a pool of over 2000 events for each of the 5 signal samples generated with top masses of 155, 165, 170, 175 and 185 GeV. In addition, samples

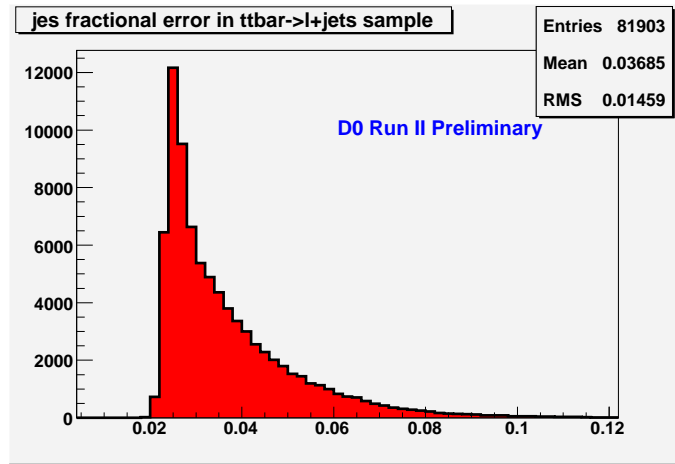


FIG. 5: Jet energy fractional error distribution for $t\bar{t}$ Monte Carlo events generated at $m_{\text{top}} = 175$ GeV. The average of this distribution was used as the width of the jet energy scale prior.

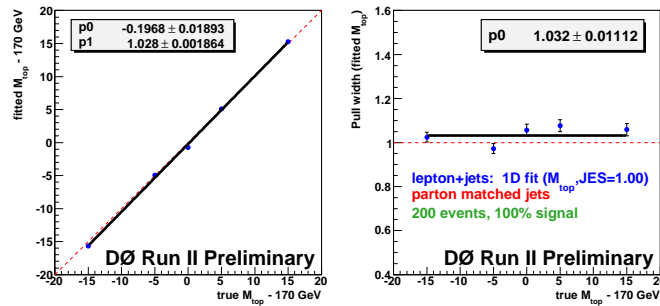


FIG. 6: Validation of the matrix element method with jet-parton matched lepton+jets $t\bar{t}$ events for a fixed JES of 1.00: Fitted m_{top} and mass pull widths are shown as a function of the input m_{top} .

with $m_{\text{top}} = 170$ GeV with all jet energies scaled by 0.95 and 1.05 are prepared in order to validate the JES fit result. m_{top} and JES are obtained for each ensemble by projecting the 2-dimensional likelihood onto the m_{top} and JES axis respectively (see Eq. 7). The results of these tests are shown in Fig. 6 for the case of a fixed JES of 1.00 (or a $\delta(JES - 1)$ prior) and in Figures 7 and 8 for the case of a flat prior in JES .

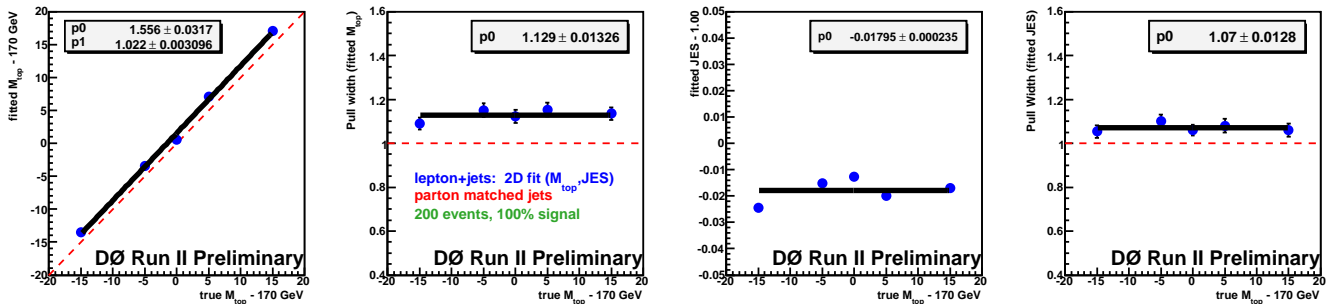


FIG. 7: Validation of the matrix element method with jet-parton matched lepton+jets $t\bar{t}$ events for an unconstrained JES : fitted m_{top} , JES , and corresponding pull widths are shown as a function of the input m_{top} .

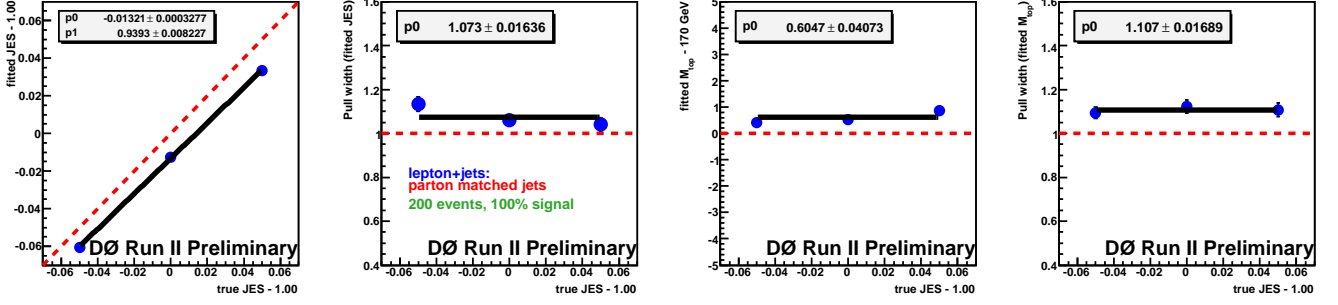


FIG. 8: Validation of the matrix element method with jet-parton matched lepton+jets $t\bar{t}$ events for an unconstrained JES : fitted m_{top} , JES , and corresponding pull widths are shown as a function of the input JES .

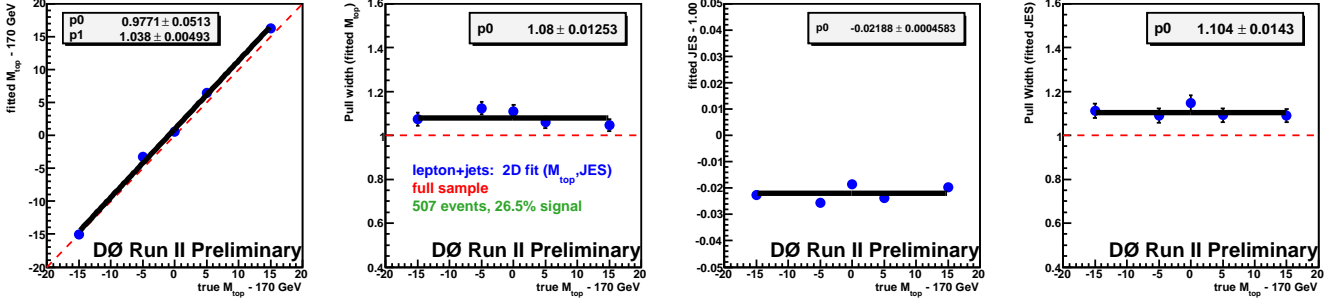


FIG. 9: Calibration of the matrix element method for lepton+jets events in the untagged analysis: fitted m_{top} , JES , and corresponding pull widths are shown as a function of the input m_{top} .

2. Calibration of the Method

Default DØ Monte Carlo events, generated as described in Section II and fed through the full simulation of the DØ detector, are found to describe the data well [6, 8]. They are therefore used to derive the final calibration of the fitting procedure. The same $t\bar{t}$ samples used for validation in Section IVC1 are used except that jets are no longer required to be matched to partons. In addition, the W +jets sample described in Section II are also used to model the background. For each sample and each lepton channel (e +jets and μ +jets), P_{sgn} and P_{bkg} are calculated for 4000 events which pass the kinematic selection. Ensembles are drawn from these event pools, with an ensemble composition as measured for the data sample (See Table I). Each probability is normalized according to the flavor of the isolated lepton. The QCD contribution is not added during the calibration but treated as a systematic uncertainty (cf. Section V).

In the untagged analysis, ensemble testing was performed with and without resampling, that is allowing (or not allowing) the same event to enter the same pseudo-experiment more than once. The calibration curves were derived separately and then applied to data. The difference between doing it one way or the other is a shift of 0.1 GeV in the final result which is negligible compared with systematic error of 1.4 GeV shown in Table III. In the b -tagged analysis, ensemble testing was performed with resampling.

For the untagged analysis, the calibration results for the fit to the combined e +jets and μ +jets ensembles are shown in Figure 9. The JES calibration plots are not shown because, due to limited computer resources, the calculation of the signal probabilities did not extend far enough in JES to keep the likelihood distributions of the JES shifted samples from being truncated at the edges of the calculated range. This range will be extended as CPU resources become available.

For the b -tagged analysis, the calibration results for the fit to the ensembles are shown separately for the e +jets and μ +jets samples in Figures 10, 11, and 12.

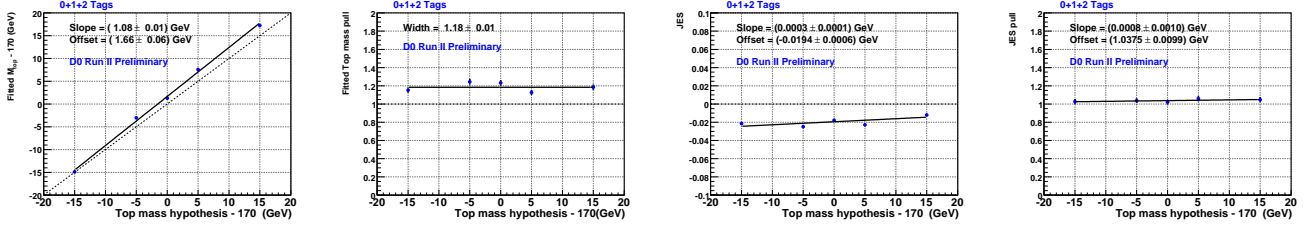


FIG. 10: Calibration of the matrix element method for e +jets events in the b -tagging analysis: fitted m_{top} , JES , and corresponding pull widths are shown as a function of the input m_{top} .

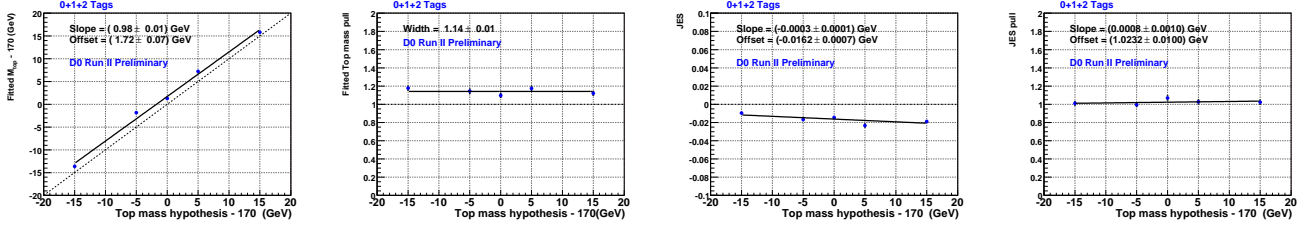


FIG. 11: Calibration of the matrix element method for μ +jets events in the b -tagging analysis: fitted m_{top} , JES , and corresponding pull widths are shown as a function of the input m_{top} .

D. Result

The matrix element method is applied to the 910 (e +jets) and 870 (μ +jets) pb^{-1} ℓ +jets data set. The calibrations for m_{top} derived in the previous section are taken into account.

The fit results for the combined ℓ +jets sample in the untagged analysis are shown in Figure 13. Only the results for m_{top} and $\sigma(m_{\text{top}})$ are calibrated. The distribution of fitted uncertainties in m_{top} is inflated by the mass pull width of 1.08 determined from the calibration plot in Figure 9. The fitted uncertainty from data is inflated by the same amount and is consistent with the expectation. No calibration is applied to the fit results for JES due to the reason described IV C 2.

For the untagged analysis, the top mass is measured to be:

$$m_{\text{top}}^{\ell+\text{jets}}(\text{topo}) = 170.5 \pm 2.5(\text{stat} + \text{JES})\text{GeV} \quad (16)$$

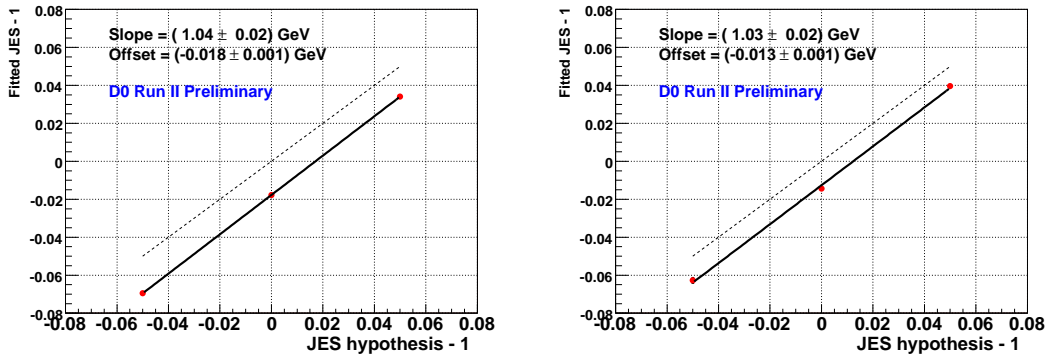


FIG. 12: Calibration of the matrix element method for e +jets (left) and μ +jets (right) events in the b -tagging analysis: fitted JES is shown as a function of the input JES .

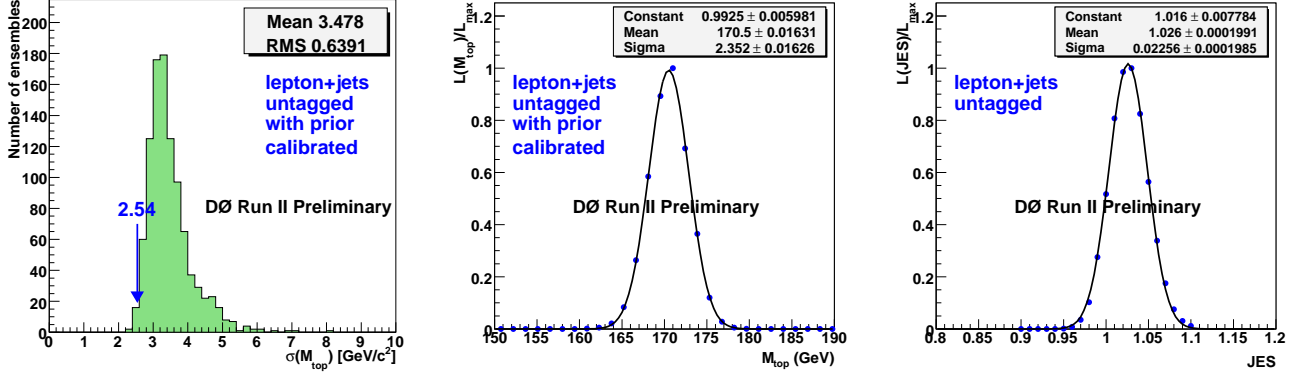


FIG. 13: Application of the untagged matrix element method to the data. The plot on the left shows the distribution of the fitted uncertainty obtained from ensemble tests done on the $m_{\text{top}} = 170$ GeV Monte Carlo sample used to derive the mass calibration. The uncertainty in data is indicated by the arrow. All uncertainties in this plot have been inflated by the width of the mass pull distributions. The center plot shows the probability as a function of the assumed m_{top} . The m_{top} axis in this plot corresponds to the calibrated values. The plot on the right shows the probability as a function of JES . Unlike the first two plots, the JES axis in this plot does not correspond to the calibrated values and the JES prior is not applied.

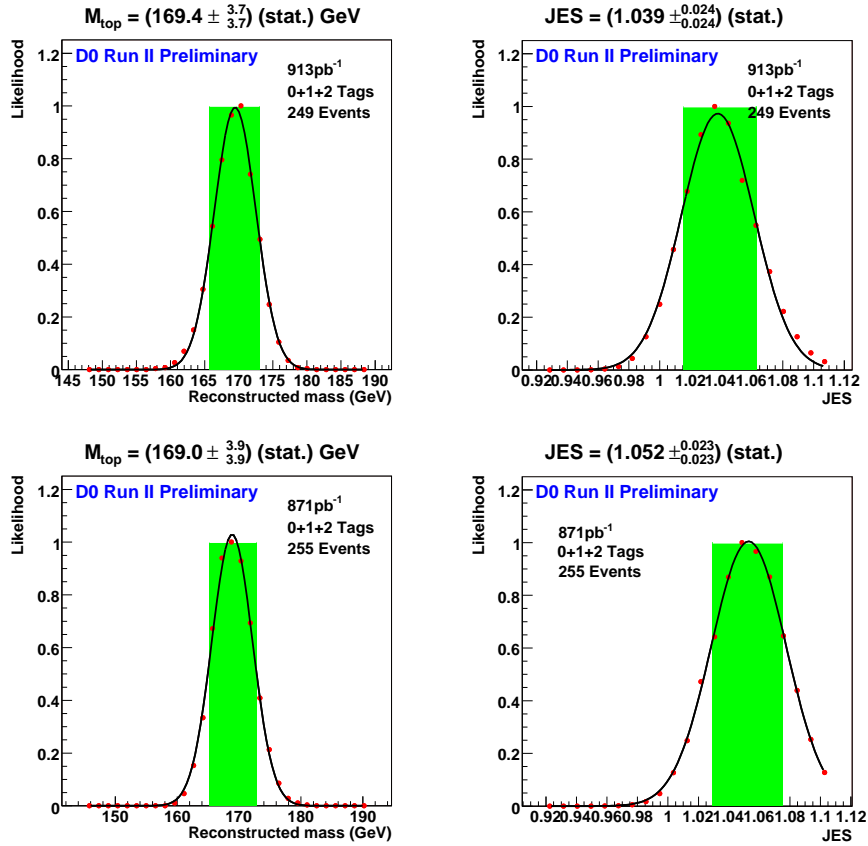


FIG. 14: Application of the b -tagging matrix element method to the data for the combined 0+1+2 tag sample before using a JES prior. The top (bottom) plots correspond to the e +jets (μ +jets) channel. The two plots on the left show the normalized likelihood as a function of the calibrated values of m_{top} . The two plots on the right show the normalized likelihood as a function of the JES parameter.

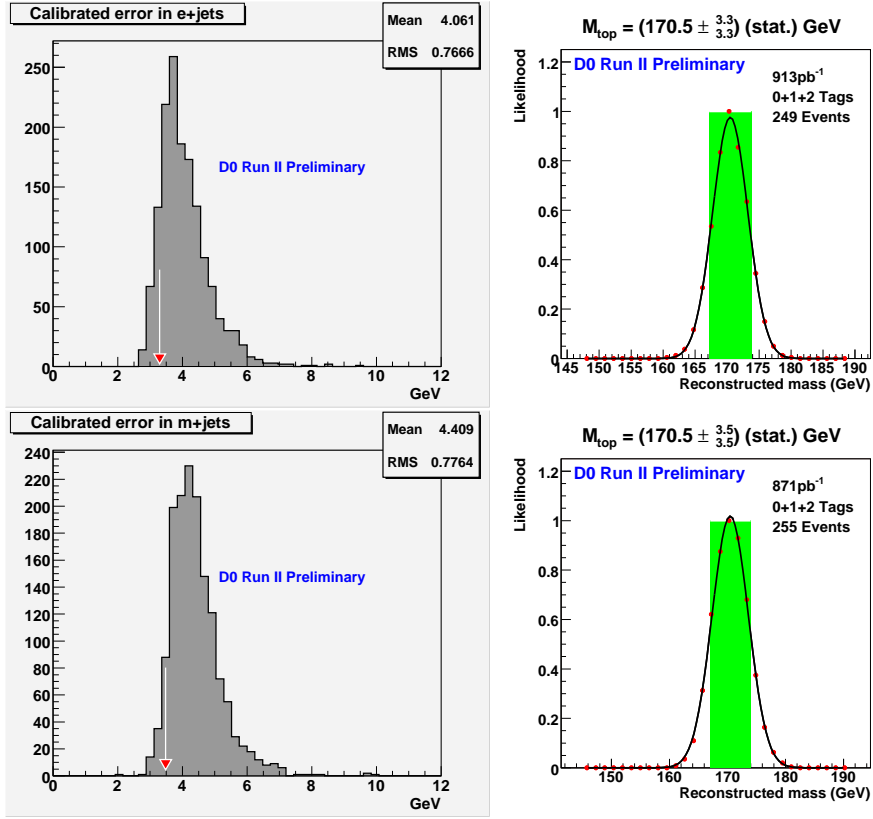


FIG. 15: Application of the b -tagging matrix element method to the data for the combined 0+1+2 tag sample using a JES Gaussian prior as described in the text. The two plots on the left show the distribution of the fitted uncertainty obtained from ensemble tests done on the $m_{\text{top}} = 170$ GeV Monte Carlo sample used to derive the mass calibration for the e +jets and μ +jets channels, respectively. The uncertainties in data are indicated by the arrows. The two plots on the right show the probability of the assumed m_{top} for the e +jets and μ +jets channels, respectively. The m_{top} axes in these plots correspond to the calibrated values.

The result without using a jet energy prior is $169.3 \pm 3.0(\text{stat} + \text{JES})\text{GeV}$.

The fit results for the b -tagged analysis are shown separately for the e +jets and μ +jets channels in Fig. 14 for the 0+1+2 tag samples without using a prior. The results after a jet energy prior is used are shown in Fig. 15. For the b -tagged analysis, the measured top mass for the 0+1+2 samples after applying a prior are:

$$\begin{aligned}
 m_{\text{top}}^{e+\text{jets}}(b\text{-tag}, 0+1+2) &= 170.5 \pm 3.3(\text{stat} + \text{JES})\text{GeV}; \\
 m_{\text{top}}^{\mu+\text{jets}}(b\text{-tag}, 0+1+2) &= 170.5 \pm 3.5(\text{stat} + \text{JES})\text{GeV}; \\
 m_{\text{top}}^{\ell+\text{jets}}(b\text{-tag}, 0+1+2) &= 170.5 \pm 2.4(\text{stat} + \text{JES})\text{GeV}.
 \end{aligned}
 \tag{17}$$

Fig. 16 shows the expected distribution of Monte Carlo errors for the combined e +jets and μ +jets samples. The arrow is the error observed in data. Fig. 17 shows the calibrated two dimensional (JES vs m_{top}) likelihoods (using the prior). The top mass and JES values are extracted by projecting these distributions onto the respective axis.

V. SYSTEMATIC ERRORS

Systematic uncertainty arises from three sources: modeling of the physics processes for $t\bar{t}$ production and background, modeling of the detector performance, and uncertainties in the methods themselves. Table III lists all uncertainties. The jet energy scale uncertainty is included in the statistical error. The total systematic uncertainty on the top mass measurement is obtained by adding all contributions in quadrature. In general, to evaluate systematic

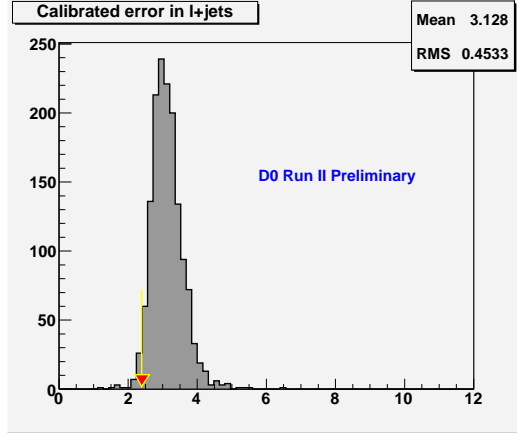


FIG. 16: Expected distribution of top mass Monte Carlo errors for the combined e +jets and μ +jets samples. The arrow shows the error observed in the data.

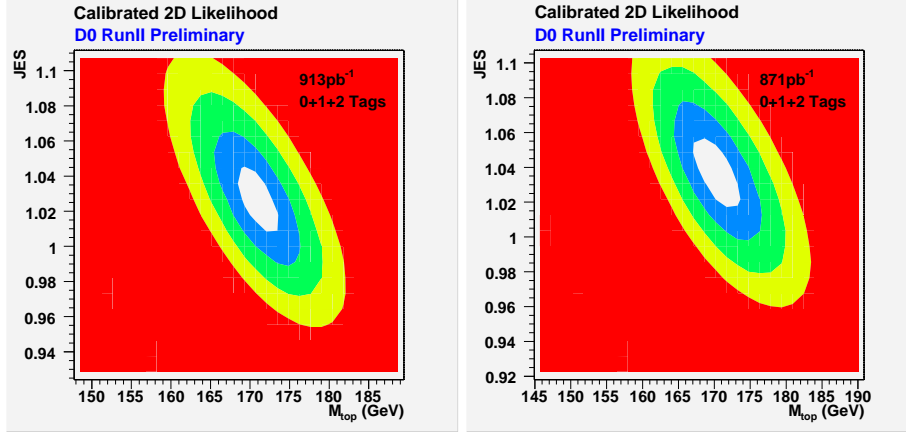


FIG. 17: Calibrated two dimensional likelihoods (using the prior). Left plot for e + jets, right plot for μ + jets. The colors show one sigma contours.

uncertainties, the simulation of events used to calibrate the measurement has been varied, while the measurement method itself has been kept unchanged.

A. Physics Modeling

- Signal modeling:** The Monte Carlo $t\bar{t}$ signal events used for validating and calibrating the method were generated with PYTHIA Tune A. To assess the systematic effect on the measured top mass due to uncertainties in signal modeling, a second sample generated with PYTHIA Tune DW was used. Both PYTHIA Tunes are described in Ref. [16]. Tune DW includes an alternative modeling of the underlying event and initial and final state radiation. Top mass measurement is sensitive to gluon radiation. The additional jets from this radiation can be confused with those coming from top or antitop decay and thus bias the top mass. The effect is minimized by requiring that events contain four and only four jets in the final state, yet situations are possible when jets from decay products are lost and replaced by initial or final state radiation jets. Ensemble tests were performed on both Tune A and Tune DW samples using only signal events generated with $m_{\text{top}} = 170$ GeV and the difference in the fitted m_{top} between the samples is taken as a systematic uncertainty.
- Background modeling:** In order to study the sensitivity of the measurement to the choice of background model, the standard W +jets Monte Carlo sample is reweighted to simulate the effect of using alternative factorization scales in the generation of these events [22]. The ensemble test done for the $m_{\text{top}} = 170$ GeV mass

Error Source	Topological Analysis	b Tagging Analysis
statistical error and jet energy scale	± 2.5	± 2.4
<i>physics modeling:</i>		
signal modeling	± 0.98	± 0.45
background modeling	± 0.47	± 0.15
PDF uncertainty	+0.26 - 0.40	+0.26 - 0.40
b fragmentation	± 0.14	± 0.54
b/c semileptonic decays	+0.06 - 0.07	± 0.05
<i>detector modeling:</i>		
JES p_T dependence	± 0.14	± 0.23
b response (h/e)	± 0.71	± 0.57
trigger	± 0.08	± 0.08
<i>method:</i>		
signal fraction	± 0.15	+0.53 - 0.24
QCD contamination	± 0.16	± 0.21
MC calibration	± 0.06	± 0.07
b -tagging		± 0.29
total systematic error	± 1.4	± 1.2
total error	± 2.9	± 2.7

TABLE III: Summary of uncertainties on the top quark mass. All errors are quoted in GeV.

point in the calibration of the method is repeated using the reweighted W +jets events and the difference in the fitted m_{top} compared with that done using the default weights is taken as a systematic uncertainty.

- **PDF uncertainty:** For this systematic uncertainty, we simply quote the value +0.26 - 0.40 GeV obtained in the P14 analysis. Leading-order matrix elements are used to calculate both P_{sgn} and P_{bkg} . Consequently, both calculations utilize a leading order parton distribution function (PDF). To study the systematic uncertainty on m_{top} due to this choice, the variations provided with the next-to-leading-order PDF set CTEQ6M [18] are used.
- **b fragmentation:** While the overall jet energy scale uncertainty is included in the statistical uncertainty from the fit, differences in the b /light jet energy scale ratio between data and simulation may still affect the measurement. Possible effects from such differences are studied by reweighting the simulated $t\bar{t}$ events used in the calibration of the method to simulate the choice of other fragmentation models for the b jets. The $t\bar{t}$ events for $m_{\text{top}} = 170$ GeV which were generated using the default Bowler [19] scheme were reweighted according to the ALEPH, DELPHI, and OPAL tune (ADO) [21]. Ensemble tests were repeated using the reweighted events and the difference in the fitted m_{top} is taken as a systematic uncertainty.
- **b/c semileptonic decays:** The reconstructed energy of b jets containing a semileptonic bottom or charm decay is in general lower than that of jets containing only hadronic decays. This can only be taken into account for jets in which a soft muon is reconstructed. Thus, the fitted top quark mass still depends on the semileptonic b and c decay branching ratios. They have been varied by reweighting events in one large ensemble of simulated events within the bounds given in [23].

B. Detector Modeling

- **JES p_T dependence:** The relative difference between the jet energy scales in data and Monte Carlo is fitted with a global scale factor, and the corresponding uncertainty is included in the quoted (stat. + JES) error. Any discrepancy between data and simulation other than a global scale difference may lead to an additional uncertainty on the top quark mass. To estimate this error, the energies of jets in the $m_{\text{top}} = 170$ GeV Monte Carlo sample used in the calibration of the method was scaled by a factor corresponding to the Jet Energy Scale uncertainty for that jet according to a parameterization in p_T and η determined from the sample. Two large

ensembles were then formed for the default sample and the one with the shifted jets, and the difference in the fitted m_{top} between the two is taken as the systematic error.

- **Relative b /light jet energy scale:** Variations of the h/e calorimeter response lead to differences in the b /light jet energy scale ratio between data and simulation in addition to the variations of the b fragmentation function considered in Section V A. Since this difference is estimated to be 1.5%, all jets that can be matched to a b parton in the $m_{\text{top}} = 170$ GeV $t\bar{t}$ Monte Carlo sample used in the calibration were scaled by this amount. Two large ensembles were then formed, one for the default sample and one with the scaled b jets and the difference in the fitted m_{top} is taken as the systematic uncertainty.
- **Trigger:** The trigger efficiencies used in composing ensembles for the calibration of the measurement are varied by their errors, and the uncertainties from all variations are summed in quadrature.

Note that no systematic uncertainty is quoted due to multiple interactions/uranium noise as opposed to the Run I measurement. The effect is much smaller in Run II as a consequence of the reduced integration time in the calorimeter readout. It is moreover covered by the jet energy scale uncertainty, as the offset correction is computed separately for data and Monte Carlo in Run II, accounting for effects arising from electronic noise and pileup.

C. Method

- **Signal fraction:** The signal fractions used for the sample compositions in the ensemble tests performed to calibrate the method are determined from a topological likelihood fit to the data. Since the uncertainties on these fractions are not insignificant, the ensemble tests are repeated by varying these fractions within the uncertainties determined from the fit. The resulting variation of the top mass is then taken as systematic uncertainty.
- **QCD background:** The W +jets simulation is used to model the small QCD background in the selected event sample in the analysis. The systematic uncertainty from this assumption is computed by selecting a dedicated QCD-enriched sample of events from data by inverting the lepton isolation cut in the event selection. The ensemble test done at $m_{\text{top}} = 170$ GeV in the calibration of the method was repeated with this QCD-enriched sample included in the composition. The difference in the fitted m_{top} when this background sample is included is taken as the systematic uncertainty.
- **MC calibration:** This systematic uncertainty is estimated by varying the calibration of the top mass measurement according to the statistical uncertainty of the calibration curve shown in Figures 10 and 11.

VI. RESULT AND CONCLUSIONS

A measurement of the top quark mass using matrix element method is presented. The purity of the lepton+jets sample is enhanced by the application of a neural-net based b -tagging technique. The data set corresponds to 0.9 fb^{-1} . The new developments in the method application are

- addition of integration over electron resolution (previously only muon resolution was taken into the account);
- integration over transverse momentum of the $t\bar{t}$ system, which was assumed to be equal to zero previously;
- Jet energies are constrained to the value derived on photon+jets sample within its uncertainty, while the hadronic W -boson mass is used as an additional constraint. In the previous version of the analysis, the jet energy scale was determined only by the hadronic W -boson mass.

The combination of the e +jets and μ +jets channels for the untagged analysis yields:

$$m_{\text{top}}(\text{topo}) = 170.5 \pm 2.5(\text{stat} + \text{JES}) \pm 1.4(\text{syst}) \text{ GeV}.$$

The combination of the e +jets and μ +jets channels for the analysis, where b -tagging information is used, yields:

$$\begin{aligned} m_{\text{top}}(b\text{-tag}) &= 170.5 \pm 2.4(\text{stat} + \text{JES}) \pm 1.2(\text{syst}) \text{ GeV}. \\ &= 170.5 \pm 1.8(\text{stat}) \pm 1.6(\text{JES}) \pm 1.2(\text{syst}) \text{ GeV}. \end{aligned} \tag{18}$$

The comparison between the results presented here and the 0.4 fb^{-1} results published in Ref. [2] for the untagged analysis are:

$$\begin{aligned} \text{PRD} : m_{\text{top}}(\text{topo}) &= 169.2_{-7.4}^{+5.0}(\text{stat} + \text{JES}) \text{ GeV}; \\ \text{this note} : m_{\text{top}}(\text{topo}) &= 170.5 \pm 2.5(\text{stat} + \text{JES}) \pm 1.4(\text{syst}) \text{ GeV}. \end{aligned} \quad (19)$$

A comparison between the previous result described in Ref. [2] and the current 0.9 fb^{-1} result without a prior ($169.3 \pm 3.0(\text{stat} + \text{JES})$) shows that on average, the uncertainty decreased by a factor of 2 which is equivalent to a factor of 4 increase in statistics.

For the b -tagged analysis, the comparison is:

$$\begin{aligned} \text{PRD} : m_{\text{top}}(b\text{-tag}) &= 170.3_{-4.5}^{+4.1}(\text{stat} + \text{JES}) \text{ GeV}; \\ \text{this note} : m_{\text{top}}(b\text{-tag}) &= 170.5 \pm 2.4(\text{stat} + \text{JES}) \text{ GeV}. \end{aligned} \quad (20)$$

Comparing the b -tagged result described in Ref. [2] with the current b -tagged analysis without using a JES prior ($169.2 \pm 2.7(\text{stat} + \text{JES})$), we see that the reduction on the error corresponds approximately to what is expected from a doubling of the data sample.

-
- [1] G. Blazey, *et al.*, *Run II Jet Physics*, DØ note 3750 (2000).
 - [2] V.M. Abazov *et al.* [DØ Collaboration], *Measurement of the top quark mass in the lepton+jets final state with the matrix element method*, Phys. Rev. D74, 092005 (2006).
 - [3] V.M. Abazov *et al.* [DØ Collaboration], *Measurement of the top quark mass in the lepton+jets channel using the ideogram method*, Fermilab-Pub-07/039-E.
 - [4] V.M. Abazov *et al.*, *A precision measurement of the mass of the Top quark*, Nature 429:638-642 (2004).
 - [5] More information on the P17 D0 reconstruction software can be found at the DØ website. Available at: <http://www-d0.fnal.gov/computing/reprocessing>.
 - [6] V.M. Abazov *et al.* [DØ Collaboration], *Measurement of the $t\bar{t}$ Production Cross Section at $\sqrt{s} = 1.96 \text{ TeV}$ in Lepton+Jets Events using Topological Method on 1fb^{-1} of D0 data*, (approved October 2006). Available at: http://www-d0.fnal.gov/Run2Physics/top/d0_private/top_private_web_pages/top_internal_review.html.
 - [7] Miruna Anastasoae, Stephen Robinson, Tim Scanlon, *Performance of the NN b -tagging Tool on p17 Data*, DØ Note 5213 (2006).
 - [8] V.M. Abazov *et al.* [DØ Collaboration], *Measurement of the $t\bar{t}$ Production Cross Section at $\sqrt{s} = 1.96 \text{ TeV}$ in Lepton+Jets Events using Secondary Vertex B -tagging*, (under review for Moriond 2007). Available at: http://www-d0.fnal.gov/Run2Physics/top/d0_private/top_private_web_pages/top_internal_review.html.
 - [9] T. Sjostrand *et al.*, Comp. Phys. Commun. **135**, 238 (2001).
 - [10] M.L. Mangano *et al.*, *ALPGEN, a Generator for Hard Multiparton Processes in Hadronic Collisions*, JHEP 307, 1 (2003).
 - [11] DØ Collaboration (V. M. Abazov *et al.*), *Measurement of the $t\bar{t}$ Production Cross Section in $p\bar{p}$ Collisions at $\sqrt{s} = 1.96 \text{ TeV}$ Using Kinematic Characteristics of Lepton+Jets Events*, FERMILAB-PUB-05-079-E (Apr 2005), hep-ex/0504043.
 - [12] G. Mahlon, S. Parke, *Maximizing Spin Correlations on Top Quark Pair Production at the Tevatron*, Phys. Lett. 80, 2063 (1997).
 - [13] S. Eidelman *et al.*, *The Review of Particle Physics*, Phys. Lett. B592, 1 (2004).
 - [14] F.A. Berends, H. Kuijf, B. Tausk, W.T. Giele, *On the Production of a W and Jets at Hadron Colliders*, Nucl. Phys. B357:32-64 (1991).
 - [15] Private communication with L. Wang. Parameterization can found in the file: `/work/cole-clued0/leiwang/wz_epmcs/p170303_sampling/wz_epmcs/src/pmcsana.cpp`.
 - [16] R. Field, *CDF Run2 Monte Carlo Tunes*. Available at: www-cdf.fnal.gov/physics/conferences/cdf8547_RDF_Tev4LHC.pdf.
 - [17] H. L. Lai *et al.* [CTEQ Collaboration], *Global QCD analysis of parton structure of the nucleon: CTEQ5 parton distributions*, Eur. Phys. J. C 12, 375 (2000).
 - [18] J. Pumplin *et al.*, *New Generation of Parton Distributions with Uncertainties from Global QCD Analysis*, JHEP 0207, 012 (2002).
 - [19] M.G. Bowler, *e^+e^- Production of Heavy Quarks in the String Model.*, Z. Phys C11, 169 (1981).
 - [20] C. Peterson *et. al.*, *Scaling Violations in Inclusive e^+e^- Annihilation Spectra.*, Phys. Rev. D27, 105 (1983).
 - [21] Y. Peters *et. al.*, *Reweighting of the Fragmentation Function for the DØ Monte Carlo*, DØ Note 5325 (2007).
 - [22] Y. Peters *et. al.*, *Factorization Scale, Estimate of Weights and Uncertainty*, Presentation given at DØ Top group meeting (2007).

- [23] The ALEPH, DELPHI, L3, OPAL, and SLD Collaborations, the LEP Electroweak Working Group, SLD Electroweak Group, and SLD Heavy Flavour Group, *Precision Electroweak Measurements on the Z Resonance*, SLAC-R-774, (2005), hep-ex/0509008.